Completing the bedrock mapping of southern Baffin Island, Nunavut: plutonic suites and regional stratigraphy

O.M. Weller[1], B.J. Dyck[2], M.R. St-Onge[3], N.M. Rayner[3] and V. Tschirhart[3]

[1]*Natural Resources Canada, Geological Survey of Canada, Ottawa, Ontario, owen.weller@canada.ca*

[2]*Department of Earth Sciences, University of Oxford, Oxford, United Kingdom*

[3]*Natural Resources Canada, Geological Survey of Canada, Ottawa, Ontario*

This work is part of the larger South Baffin mapping project, a partnership between the Canada-Nunavut Geoscience Office (CNGO) and Natural Resources Canada's (NRCan) Geo-mapping for Energy and Minerals (GEM) program on Baffin Island. This particular mapping project is being led by the Geological Survey of Canada (GSC) in collaboration with CNGO, the Government of Nunavut, Nunavut Arctic College, Carleton University and Oxford University. Logistical support is provided by the Polar Continental Shelf Project and several, local, Inuit-owned businesses. The study area comprises all or parts of six 1:250 000 map areas north of Iqaluit (NTS areas 26B, C, F, G, J and K). The objective of the work is to complete the regional bedrock mapping for the southern half of Baffin Island and provide a new, modern, geoscience understanding of this part of eastern Nunavut.

Weller, O.M., Dyck, B.J., St-Onge, M.R., Rayner, N.M. and Tschirhart, V. 2015: Completing the bedrock mapping of southern Baffin Island, Nunavut: plutonic suites and regional stratigraphy; *in* Summary of Activities 2015, Canada-Nunavut Geoscience Office, p. 33–48.

Abstract

This paper summarizes the field observations and initial interpretations following eight weeks of regional and targeted bedrock mapping on south-central Baffin Island, Nunavut. The 2015 field campaign completes a two-decade mission to update the geoscience knowledge for the whole of Baffin Island south of latitude 70°N. The bedrock in the area is dominated by a Paleoproterozoic metaplutonic suite, ranging in composition from gabbro to syenogranite, with crosscutting relations indicating a progression from mafic to silicic magmatism. Phase-equilibria modelling reveals that the prevailing upper-amphibolite– to lower-granulite–facies metamorphic conditions overlap the stability limits of magnetite and orthopyroxene for a typical granitoid bulk composition, which is consistent with field observations of the discontinuous presence of both phases throughout the map area. This result is also consistent with regional aeromagnetic data that show complex structures within relatively homogeneous map units, which are primarily attributed to variations in the abundance of magnetite. The granitoid rocks are interpreted as part of the middle Paleoproterozoic Cumberland Batholith.

Metasedimentary rocks, including quartzite, pelite, marble and metagreywacke, are present as enclaves and screens within and between plutonic bodies. An examination of the 'ghost' stratigraphy suggests that the metasedimentary rocks throughout most of the map area can be correlated with the middle Paleoproterozoic Lake Harbour Group, except in the northeast, where the unique presence of greywacke suggests a middle Paleoproterozoic Piling Group affinity. This transition in strata is consistent with the proposal that a middle Paleoproterozoic tectonic suture (the Baffin suture) associated with the Trans-Hudson Orogen runs through Cumberland Sound. Completion of the bedrock mapping in southern Baffin Island indicates that the region offers a world-class exposure of a reworked Paleoproterozoic convergent margin, which affords valuable insight into a variety of magmatic and tectonic processes that can be applied to younger collisional belts.

Résumé

Le présent rapport résume les observations de terrain et les interprétations préliminaires à la suite de huit semaines de cartographie régionale et ciblée de la roche en place dans la partie centre-sud de l'île de Baffin, au Nunavut. La campagne de terrain 2015 achève deux décennies de travaux ayant pour objet la mise à jour des connaissances géoscientifiques pour l'ensemble de l'île de Baffin gisant au sud de la latitude 70°N. Le socle rocheux dans la région est constitué d'une suite métaplutonique d'âge paléoprotérozoïque, dont la composition varie du gabbro au granite syénitique ; les relations de recoupement qui la caractérisent attestent de la progression des épisodes de magmatisme de nature mafique à siliceuse. La modélisation de diagrammes de phases révèle que les conditions métamorphiques du faciès des amphibolites supérieur au faciès des granulites inférieur chevauchent les limites de stabilité typiques de la magnétite et de l'orthopyroxène pour une

This publication is also available, free of charge, as colour digital files in Adobe Acrobat® PDF format from the Canada-Nunavut Geoscience Office website: http://cngo.ca/summary-of-activities/2015/.

composition granitique caractéristique, ce qui concorde avec les observations de terrain et la présence discontinue des deux phases dans l'ensemble de la région à l'étude. Ce résultat est également compatible avec les données aéromagnétiques régionales qui montrent des structures complexes au sein d'unités cartographiques relativement homogènes, structures dont l'identification est principalement attribuable à la présence de quantités variables de magnétite. Les roches granitoïdes sont interprétées comme faisant partie du batholite de Cumberland datant du Paléoprotérozoïque moyen.

Des roches métasédimentaires, y compris du quartzite, de la pélite, du marbre et de la métagrauwacke, sont présents sous forme d'écrans et d'enclaves entre des masses plutoniques et au sein de ces dernières. Un examen de la stratigraphie «fantôme» semble indiquer que les roches métasédimentaires dans presque l'ensemble de la région cartographiée peuvent être mises en corrélation avec celles du groupe de Lake Harbour datant du Paléoprotérozoïque moyen, sauf dans le nord-est, où la présence unique de grauwacke semble indiquer une affinité avec le groupe de Piling, datant lui aussi du Paléoprotérozoïque moyen. Cette transition concorde avec la proposition selon laquelle une suture tectonique datant du Paléoprotérozoïque moyen (la suture de Baffin), associée à l'orogénie Trans-hudsonienne, traverse le détroit de Cumberland. L'achèvement des travaux de cartographie du substratum rocheux dans le sud de l'île de Baffin révèle une région offrant un exemple frappant d'une marge convergente retravaillée d'âge paléoprotérozoïque, susceptible de livrer de précieux renseignements au sujet d'une variété de processus magmatiques et tectoniques qui peuvent être appliqués aux chaînes de collision plus récentes.

Introduction

Natural Resources Canada's (NRCan) Geo-mapping for Energy and Minerals (GEM) program targeted south-central Baffin Island for strategic, helicopter-assisted bedrock mapping in 2015 (red polygon, Figure 1). The GEM program provides modern, publicly available, regional-scale geoscience knowledge of Canada's North, which supports evidence-based exploration for new energy and mineral resources and enables northern communities to make informed decisions about their land, economy and society. The 2015 field campaign was particularly significant as it updates the regional bedrock-mapping coverage for the southern half of Baffin Island (south of latitude 70°N), allowing for a new, modern, geoscience compilation of the area. Fieldwork in the region (parts of NTS map areas 26B, C, F, G, J and K) was led by the Geological Survey of Canada (GSC) in collaboration with the Canada-Nunavut Geoscience Office (CNGO), and also involved participants from Nunavut Arctic College, Carleton University, Oxford University and the Government of Nunavut. This paper presents an overview of the regional geology, and outlines the dominant tectonostratigraphic units and economic potential identified during eight weeks of fieldwork in 2015.

Historical bedrock mapping

Initial reconnaissance geological investigations of Baffin Island south of latitude 66°N were carried out from 1949 to 1965, with the data compiled into a regional bedrock map that covered eighteen 1:250 000 NTS map areas (Blackadar, 1967). This was followed by a series of helicopter-borne operations in central Baffin Island (e.g., Henderson, 1985). More recently, modern geoscience knowledge has been provided by field campaigns featuring helicopter-assisted foot traverses in: southern Baffin Island (1995–1997; green shading in Figure 1), central Baffin Island (2000–2002; orange shading in Figure 1), south-west Baffin Island (2006; yellow shading in Figure 1), Cumberland Peninsula (2009–2011; pale pink shading in Figure 1), Hall Peninsula (2012–2014; blue shading in Figure 1) and Meta Incognita Peninsula (2014; purple shading in Figure 1). Prior to the summer of 2015, only one section remained to finalize the updated coverage of the whole of Baffin Island south of latitude 70°N: south-central Baffin Island in the Clearwater Fiord–Sylvia Grinnell Lake area (red polygon in Figure 1). This area was the focus of the 2015 field campaign and is the subject of this paper.

Geological framework

South-central Baffin Island forms part of the northeastern (Quebec–Baffin) segment of the Trans-Hudson Orogen (THO), which is a collisional belt that extends in a broad arcuate shape from north-eastern to south-central North America (Hoffman, 1988). The THO formed during the final phase of growth of the Nuna supercontinent, and *sensu lato* records the closure of the Manikewan Ocean between the lower Superior and upper Churchill plates from 1.92 to 1.80 Ga. In detail, the THO is a composite collision zone that involved a series of short-duration tectonothermal events, which encompass specific accretionary phases within a much larger orogenic system during 120 m.y. of gradual ocean-basin closure (Corrigan et al., 2009; St-Onge et al., 2009). In the southeastern Baffin region, four orogen-scale stacked tectonic levels have been identified (Figure 2). From lowest to highest structural level, these comprise

1) Archean basement orthogneiss, interpreted as the northern continuation of the Superior craton, and middle Paleoproterozoic supracrustal cover (Povungnituk Group; St-Onge et al., 1996);
2) middle Paleoproterozoic, dominantly monzogranitic and granodioritic orthogneiss, interpreted as a deformed

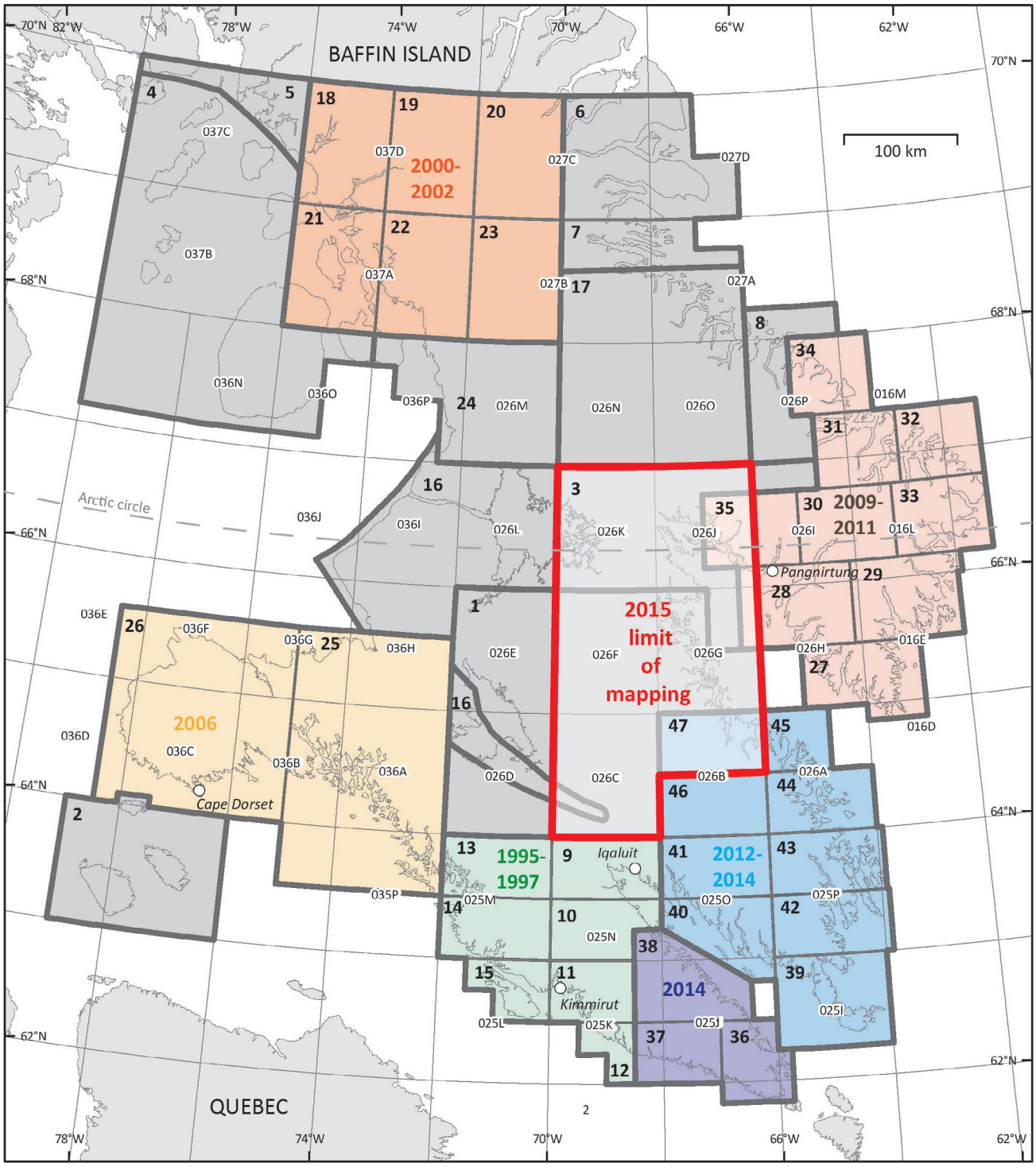

Figure 1: Summary of bedrock-mapping campaigns undertaken on Baffin Island, Nunavut. The location of the 2015 south-central Baffin Island map area is shown as a red polygon, and completes the modern mapping coverage south of 70°N. Bold numbers denote map references in chronological order, which are listed in Appendix 1. Coloured shading highlights areas and year(s) of recent field campaigns, as described in the text. Alphanumeric designators refer to NTS map areas.

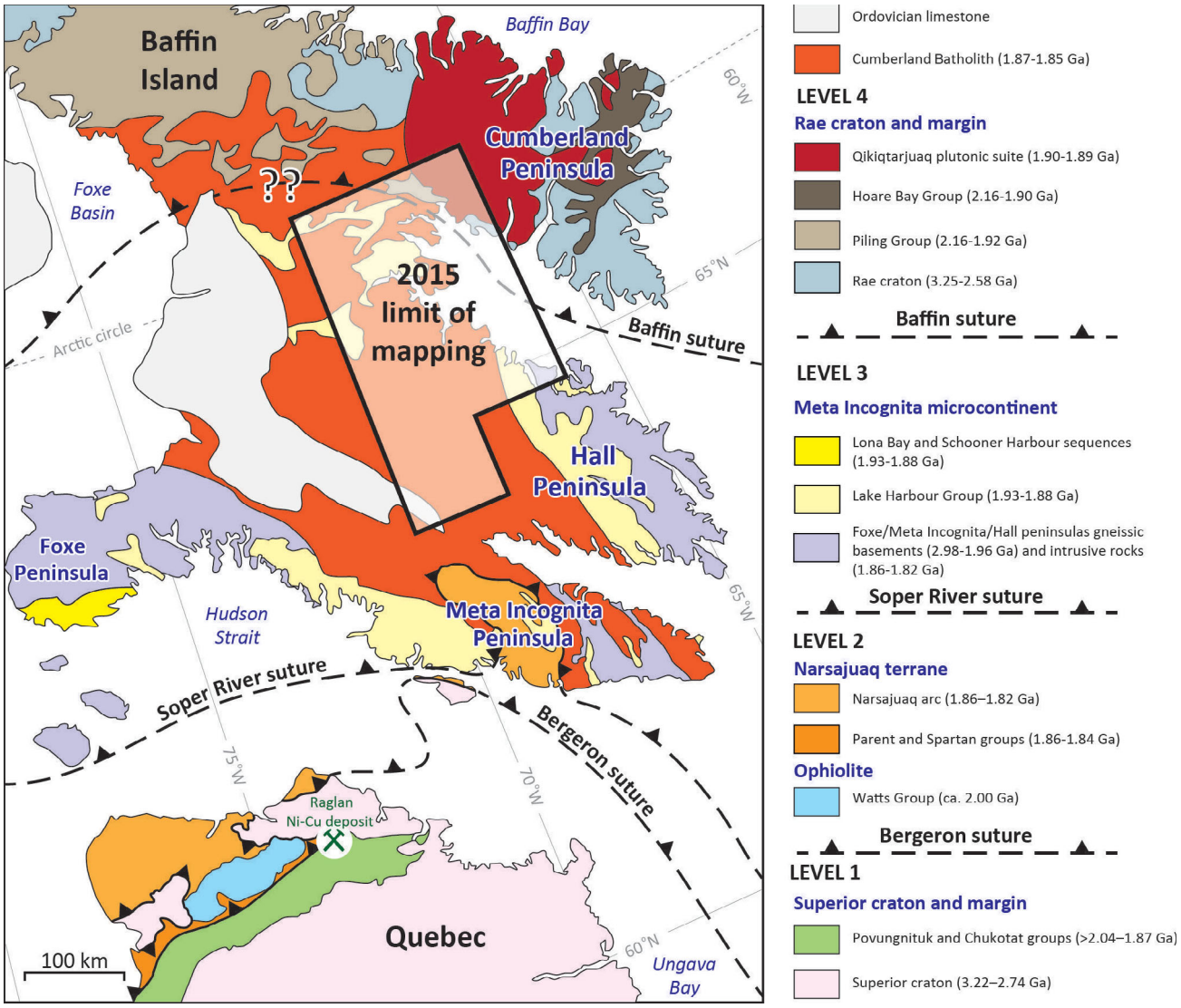

Figure 2: Simplified geological terrane map of the Quebec–Baffin segment of the Trans-Hudson Orogen (modified from St-Onge et al., 2007), showing the four structural levels and three sutures. The map provides a regional tectonic context for the south-central Baffin Island map area, which is outlined in black.

arc-magmatic terrane (Narsajuaq arc; Scott, 1997; St-Onge et al., 2009) or as Narsajuaq-age intrusions in level 3 (Corrigan et al. 2009);

3) Archean basement orthogneiss and middle Paleoproterozoic supracrustal cover (Lake Harbour Group), collectively termed the 'Meta Incognita microcontinent' by St-Onge et al. (2000a), which either represents crust rifted from the Rae or Superior cratons, or is exotic to both; and
4) Archean basement orthogneiss, interpreted as the southern continuation of the Rae craton, and middle Paleoproterozoic supracrustal cover (Piling Group; Wodicka et al., 2014), stratigraphically similar to the Hoare Bay Group on Cumberland Peninsula; both the basement and cover are intruded by a middle Paleoproterozoic felsic plutonic suite (the Qikiqtarjuaq suite; Rayner et al., 2012).

Levels 3 and 4 are pervasively intruded by the Cumberland Batholith, which comprises various granitoid phases dated at ca. 1865–1845 Ma (Whalen et al., 2010). The Cumberland Batholith has been interpreted as an Andean-type batholith (St-Onge et al., 2009), or as the result of post-collisional lithospheric delamination and mantle upwelling (Whalen et al., 2010). All levels are crosscut by ca. 720 Ma basaltic 'Franklin' dykes, which were emplaced during plume magmatism associated with the break-up of the Rodinia supercontinent (Heaman et al., 1992). Levels 3 and 4 are also unconformably overlain by Ordovician limestone strata (Blackadar, 1967).

The four tectonic elements were progressively accreted from the south across a series of north-dipping crustal sutures during long-lived deformation associated with the THO. The oldest of these sutures, the level 3–4 'Baffin suture', is pro-

posed to have resulted from accretion of the Meta Incognita microcontinent to the Rae craton at ca. 1880–1865 Ma (St-Onge et al., 2006). Evidence of this suture is relatively sparse due to postaccretion magmatism engulfing the suture zone, but includes the presence of distinct and opposite-facing stratigraphy in the region (St-Onge et al., 2009). To the north of the proposed suture is the stratigraphically south-facing Piling Group, which comprises a continental margin sequence, characterized by basal shallow-marine continental-margin clastic and carbonate-platform strata, overlain by a volcano-sedimentary rift package that includes iron formations, and capped by foredeep turbidites (Wodicka et al., 2014). To the south of the proposed suture is the north-facing Lake Harbour Group, which also comprises a clastic-carbonate continent- to foredeep-margin sequence but with notable differences, including the presence of a basal orthoquartzite and the absence of iron formation and greywacke. Further evidence for the suture includes thrust imbrication of basement-cover panels in level 3 that predate emplacement of the Cumberland Batholith (St-Onge et al., 2007). As the 2015 map area straddles the proposed Baffin suture, one of the major objectives of the campaign was to further investigate this structure.

The level 2–3 'Soper River' suture records the accretion of the Narsajuaq magmatic arc to the Rae-Meta Incognita continental margin. Formation of the suture is bracketed between ca. 1845 Ma, the age of the youngest intra-oceanic phase in the arc (Dunphy and Ludden, 1998), and ca. 1842 Ma, the age of the oldest Andean-type phase (Scott, 1997). Deformation in the hanging wall of the Soper River suture is both extensive and penetrative, and manifest as a regional synmetamorphic amphibolite- to granulite-facies metamorphic foliation (St-Onge et al., 2007).

The level 1–2 'Bergeron' suture formed during terminal collision of the Superior craton with the amalgamated mosaic of upper-plate terranes (collectively the Churchill plate or peri-Churchill collage), and is bracketed between ca. 1820 Ma, the age of the youngest dated plutonic unit in the hanging wall of the suture (Scott and Wodicka, 1998), and ca. 1795 Ma, the age of a dyke that crosscuts the suture (Wodicka and Scott, 1997). This event resulted in localized retrograde amphibolite-facies metamorphism of granulite-facies rocks in the upper plate of the collision in southern Baffin Island along reactivated Soper River structures and associated fluid-infiltration zones (St-Onge et al., 2000b).

Field observations of 2015

Bedrock mapping of the Clearwater Fiord–Sylvia Grinnell Lake area was completed during eight weeks of strategic, helicopter-assisted fieldwork in the summer of 2015. The bedrock in the area is dominated by a metaplutonic suite ranging in composition from gabbro to syenogranite (Figure 2). Crosscutting relationships define a relative chronology of emplacement for the various phases (e.g., Figure 3a), which can be broadly summarized as a transition from mafic through to more silicic compositions. A suite of samples from the various metagranitoid phases, which are described in their relative age order below, was collected for U-Pb dating to corroborate field crosscutting relationships and the likely correlation with the Cumberland Batholith. Although most of the rocks in the field area are penetratively deformed metamorphic rocks, the prefix 'meta' is omitted from the following lithological descriptions of the metagranitoid units for brevity.

Metasedimentary strata, including quartzite, semipelite, pelite, marble and metagreywacke, occur as enclaves, panels and screens within and between various plutons. Mafic-ultramafic bodies are present as sills within the metasedimentary strata. Field relationships indicate that emplacement of the sills predates emplacement of the metaplutonic suite. Lastly, minor crosscutting Neoproterozoic Franklin dykes (Heaman et al., 1992) and overlying Ordovician limestone (Blackadar, 1967) occur in the map area.

Metagranitoid units

Gabbro

A single, coarse-grained to pegmatitic, kilometre-scale, layered biotite-clinopyroxene-magnetite±hornblende gabbro pluton is present in the northwestern corner of the map area. In places, the pluton contains metre-scale lenses of clinopyroxene-bearing anorthosite.

Quartz diorite

Quartz diorite occurs as a fine-grained, dark-weathering, massive to foliated unit containing the assemblage biotite-clinopyroxene-orthopyroxene±hornblende. It is present as discrete plutons in the western part of the map area and as enclaves within all other metaplutonic units to the east (Figure 3a). Map-scale structural trends indicate that the unit occurs toward the stratigraphic base of the metaplutonic suite.

Biotite granodiorite

Minor, generally massive, biotite±hornblende±magnetite granodiorite is documented in the northwestern part of the map area. The unit is typically dark weathering and medium grained.

K-feldspar–megacrystic biotite monzogranite

Pink- to orange-weathering, medium- to coarse-grained, massive to foliated biotite±orthopyroxene±magnetite±garnet monzogranite, with distinctive K-feldspar megacrysts, occurs throughout large parts of south-central Baffin Island. Potassium-feldspar phenocrysts form augen up to 10 cm wide and locally display rapakivi textures (ovoid alkali feldspar mantled by plagioclase feldspar; Figure 3b). The unit is locally reworked by a kilometre-scale north-dipping

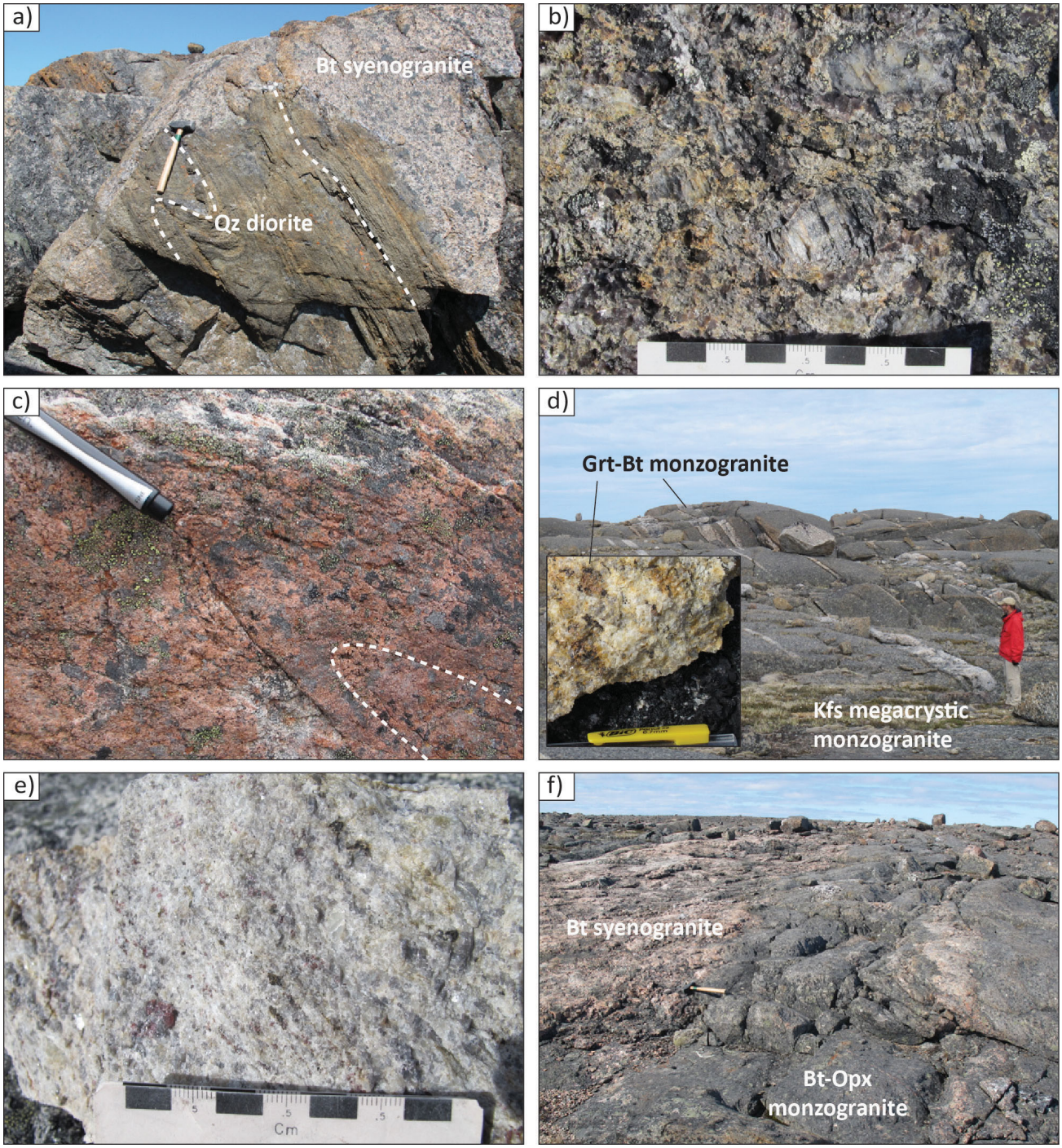

Figure 3: Representative photos of metagranitoid units from southern Baffin Island: **a)** enclave of folded and foliated quartz diorite in massive, coarse-grained biotite syenogranite; **b)** close-up of the K-feldspar–megacrystic monzogranite showing 3–6 cm zoned feldspar augen displaying rapakivi texture; **c)** isoclinally folded biotite-orthopyroxene monzogranite; **d)** massive K-feldspar–megacrystic monzogranite cut by a series of subparallel garnet-biotite monzogranite dykes (geologist for scale is 1.8 m tall); inset: close-up of a garnet-biotite monzogranite sample, showing 1–3 cm burgundy garnet phenocrysts and a weak foliation defined by subparallel biotite flakes; **e)** close-up of a garnet-sillimanite leucogranite, showing abundant pinhead-sized lilac garnet; **f)** massive biotite-orthopyroxene monzogranite cut by a network of anastomosing biotite syenogranite dykes (hammer for scale is 30 cm long). Abbreviations: Bt, biotite; Grt, garnet; Kfs, K-feldspar; Opx, orthopyroxene; Qz, quartz.

shear zone in the northern portion of the map area, with σ-porphyroclasts of K-feldspar defining a top-to-the-south thrust sense of shear.

Biotite monzogranite

Well-foliated biotite±orthopyroxene±magnetite±hornblende±garnet monzogranite underlies large parts of south-central Baffin. The unit is typically medium grained, tan to pink weathering and equigranular. The unit alternates between magnetite-rich and magnetite-free domains, and contains hornblende in the north-western part of the map area. In places, the foliation is observed to be axial planar to isoclinal folding of the unit (Figure 3c), suggestive of widespread shortening across the region.

Garnet-biotite monzogranite

White-weathering, massive to foliated, fine- to medium-grained garnet-biotite±magnetite monzogranite occurs predominantly in the eastern portion of the map area. The unit is present as dykes and sills in the K-feldspar–megacrystic monzogranite (Figure 3d) and forms plutons that intrude the biotite monzogranite. Garnet is present as abundant 2–30 mm burgundy phenocrysts, frequently in association with biotite (inset in Figure 3d).

Garnet-sillimanite leucogranite

Dykes of garnet-sillimanite leucogranite crosscut the garnet-biotite monzogranite in the eastern part of the map area. The unit is typically fine grained, with 1–5 mm lilac garnet phenocrysts and mats of sillimanite (Figure 3e). The presence of sillimanite suggests that the leucogranite is derived from muscovite-dehydration melting of metasedimentary units as documented elsewhere on southern Baffin Island (e.g., Dyck et al., 2015), rather than being a highly fractionated component of the plutonic suite.

Biotite syenogranite

Coarse-grained to pegmatitic, pink-weathering biotite syenogranite forms anastomosing dykes in most units (Figure 3f). In places the syenogranite is foliated, but typically the unit is undeformed and cuts the foliation of the hostrock (Figure 3a). Rarely, the dykes contain phenocrysts of garnet and tourmaline.

Metasedimentary units

Quartzite, psammite, semipelite and pelite

Well-layered and rusty-weathering quartzite occurs as panels up to several hundred metres thick within monzogranite (Figure 4a), and in places is overlain by interbedded psammite, semipelite and/or pelite (Figure 4b). Quartzite layers range in composition from orthoquartzite to feldspathic quartzite, are strongly recrystallized and occasionally contain garnet. Pelite horizons contain the assemblage biotite–garnet–sillimanite–K-feldspar–melt (Figure 4c), and typically occur as subordinate layers within biotite±garnet psammitic or biotite±garnet±sillimanite semipelitic migmatite. The primary assemblages contain up to 20 vol. % coarsened leucosome, interpreted as crystallized melt, with patch to stromatic metatexite textures. The assemblages are devoid of muscovite, consistent with peak metamorphic conditions that exceeded muscovite dehydration (St-Onge et al., 2007; Dyck and St-Onge, 2014). Cordierite is also absent from the metasedimentary assemblages, suggesting paleopressures in excess of 6 kbar. Gossanous horizons are common in the siliciclastic units, which locally host chalcopyrite, graphite and pyrite. Although only seen in restricted windows, the siliciclastic units across most of the map area are lithologically similar to the metasedimentary strata of the contiguous Lake Harbour Group in its type locality (St-Onge et al. 1996, 1998; Scott et al. 1997).

Marble and calcsilicate

Calcareous rocks occur as panels up to 100 m thick within the monzogranite and can be traced for up to 10 km along strike (Figure 4d). The rocks are medium to coarse grained, and locally display compositional layering defined by varying proportions of apatite, calcite, diopside, humite, forsterite, magnetite, phlogopite, scapolite, spodumene, titanite and tremolite (Figure 4e). The calcareous units are considered to represent a structurally higher part of the Lake Harbour Group than the siliciclastic units described above.

Metagreywacke

Metagreywacke was documented in one locality in the north-eastern part of the map area, occurring as enclaves within a biotite monzogranite (Figure 4f). As noted above, greywacke is not a feature of the type Lake Harbour Group stratigraphy, but is a dominant component of the Pilling Group mapped to the north, suggesting a transition in granitoid host stratigraphy.

Other units

Mafic-ultramafic sills

Sheets of medium- to coarse-grained, mafic to ultramafic rocks of the Frobisher suite (Liikane et al., 2015) occur throughout the siliciclastic strata of south-central Baffin Island. Individual bodies are typically 10–20 m thick, although some reach a few hundred metres in thickness, and extend up to several kilometres along strike. The mafic and ultramafic rocks display sharp, concordant margins with their host metasedimentary units, suggesting that they are sills. Larger bodies are compositionally layered, typified by a sequence comprising clinopyroxene-orthopyroxene± hornblende metapyroxenite at the base (Figure 5a), followed by olivine-clinopyroxene-orthopyroxene metaperidotite and metagabbro to metaleucogabbro upsection (Figure 5b). A M.Sc. thesis is currently being completed on the petrology, geochemistry and geochronology of the layered mafic-ultramafic suite and associated mineralization. One of the central questions posed by this thesis is whether the

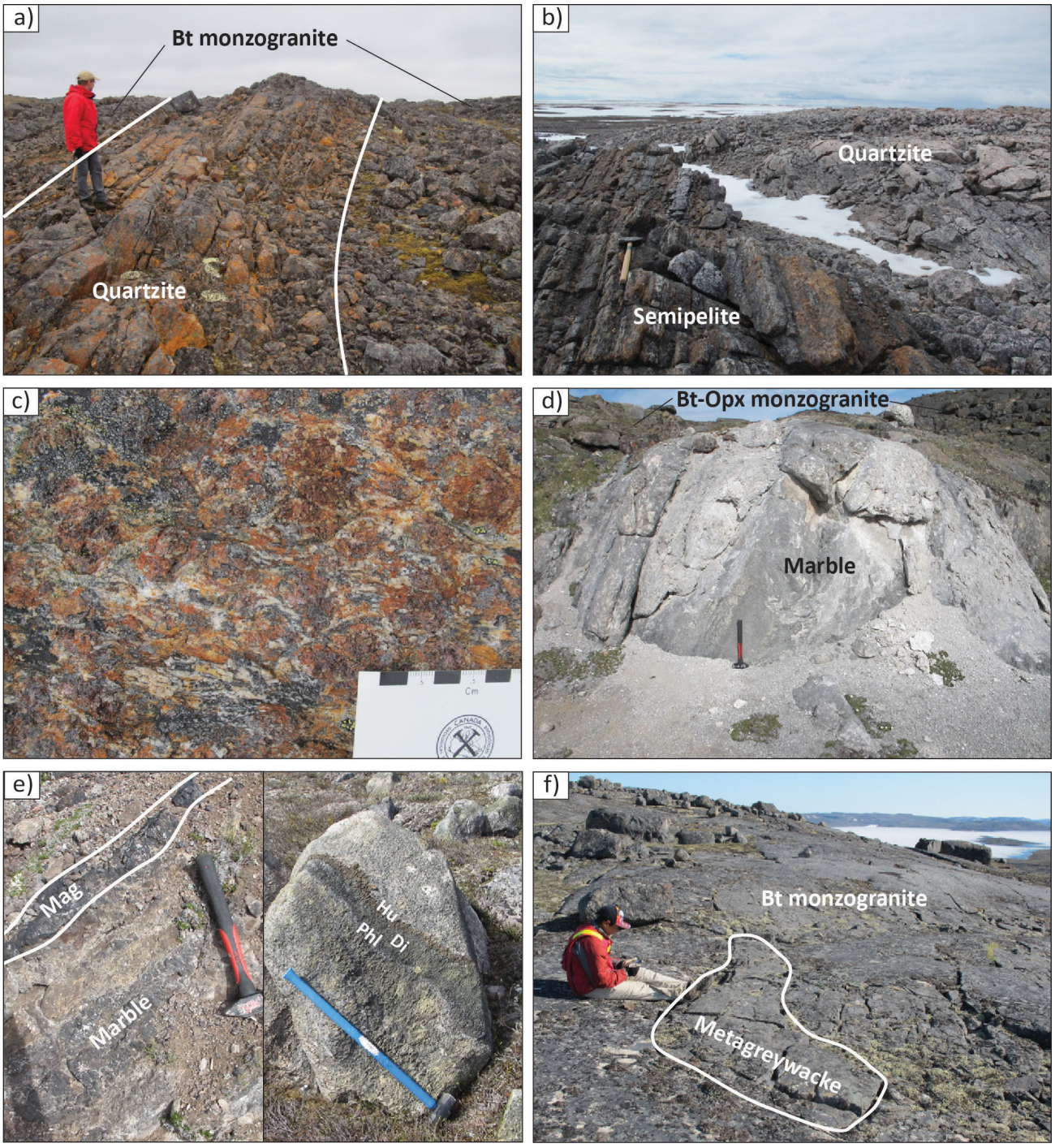

Figure 4: Representative photos of metasedimentary units on southern Baffin Island: **a)** panel of rusty-weathered quartzite 10 m wide in biotite monzogranite; **b)** well-layered quartzite interbedded with pelite/semipelite (hammer for scale is 30 cm long); **c)** close-up of the pelite/semipelite, showing 1–2 cm garnet porphyroblasts wrapped by biotite and sillimanite, which define a foliation; **d)** enclave of marble within biotite-orthopyroxene monzogranite (hammer for scale is 30 cm long); **e)** left: magnetite horizon in marble (hammer for scale is 30 cm long); right: banding in marble caused by varying amounts of humite, diopside and phlogopite (hammer for scale is 60 cm long); **f)** enclave of metagreywacke in biotite monzogranite (geologist for scale is 1.8 m tall). Abbreviations: Bt, biotite; Di, diopside; Hu, humite; Mag, magnetite; Opx, orthopyroxene; Phl, phlogopite.

suite is correlative with similar layered intrusions in northern Quebec that are associated with the Raglan Ni-Cu deposit (Figure 2). A more complete description of the mafic-ultramafic rocks is given in Liikane et al. (2015).

Basaltic dykes

A suite of minor 1–20 m wide subvertical, fine- to medium-grained basaltic dykes containing 1–2 mm plagioclase phenocrysts are present throughout south-central Baffin Island (Figure 5c). The dykes are relatively magnetic, consistently trend at 110–120° (Tschirhart et al., 2015) and are attributed to the widespread Neoproterozoic (ca. 720 Ma) Franklin dyke suite (Heaman et al., 1992).

Limestone

Shallowly dipping (<10°) limestone (Blackadar, 1967) of the middle Ordovician Amadjuak Formation (Sanford and Grant, 2000) occurs as erosional outliers in the south-western part of the map area (Figure 2). In places, the limestone is juxtaposed against the plutonic suite by northwest-striking normal faults, which were active during Paleocene rifting of the Davis Strait (Clarke et al., 1989). The limestone is typically composed of medium-grey lime mud and is fossiliferous, with the assemblage including Maclurites, gastropods, cephalopods, brachiopods, coral fragments and crinoid stems (Figure 5d).

Phase-equilibria modelling

Phase-equilibria modelling of a representative sample of the Cumberland Batholith was undertaken to investigate the competing effects of pressure, temperature and composition (P, T and X) on the metamorphic mineral assemblage. Phase relationships were calculated across a range of P-T space, centred upon documented regional metamorphic conditions of 6–8 kbar and 700–800°C (St-Onge et al., 2007), with the intent of rationalizing the range of phases documented within the metagranitoid units, rather than refining P-T estimates. All P-T and T-X phase diagrams were constructed using THERMOCALC v3.40 and the internally consistent dataset tc-ds55 updated to August, 2004 (Holland and Powell, 1998). Modelling was performed in the 11 component MnO-Na_2O-CaO-K_2O-FeO-MgO-Al_2O_3-SiO_2-H_2O-TiO_2-Fe_2O_3 system, using the high-temperature solid-solution models considered in Weller et al. (in press). Pressure uncertainties for assemblage-field boundaries are approximately ±1 kbar at the 2σ level (Powell and Holland, 2008; Palin et al., in press). Bulk compositions were calculated by modifying whole-rock X-ray fluorescence data presented by Theriault et al. (2001) for a monzogranite sampled from southern Baffin Island (sample 95-D078B), following the technique of Weller et al. (2013). Modifications included adjusting the CaO total by assuming that all P_2O_5 resided in apatite; applying a value of $XFe^{3+} = Fe^{3+}/\text{total Fe} = 0.1$, using the oxides present as a guide to oxidation state (Diener and Powell, 2010); and setting molar H_2O in the effective bulk composition (MH_2O) at 0.1%, as metagranitoid rocks are relatively anhydrous (Bucher and Frey, 2002). Both of the latter assumptions are explored using relevant T-X diagrams. All bulk compositions are listed in Table 1.

A P-T diagram calculated for a representative monzogranite sample (sample 95-D078B from Theriault et al., 2001; Figure 6a) reveals few reactions between high-variance assemblages across a wide range of P-T space, as is typical of metagranitoid rocks, with only magnetite (blue line) and orthopyroxene (green line) calculated to have limited stability over the considered subsolidus conditions. Of note, both orthopyroxene and magnetite stability limits are encountered within the P-T range of relevance to south-central Baffin Island (white dashed box), consistent with field observations of the discontinuous presence of both phases across the region.

To investigate the effects of H_2O on the assemblage, a T-MH_2O diagram was constructed at a mid-range pressure (7 kbar), with MH_2O varying from 0 to 1 mol% (Figure 6b). This diagram reveals that with increasing H_2O content, the temperature of orthopyroxene-in (green line) rapidly increases from ca. 640°C to 810°C, and conversely the solidus (orange line) decreases from ca. 810°C to 640°C. Given the relevant temperature range of 600–800°C, the presence of orthopyroxene and absence of partial melt textures in the metagranitoid rocks suggest that the assumption of a relatively anhydrous bulk composition (0.1 mol% H_2O, Table 1; white dashed line in Figure 6b) is appropriate. This result is also consistent with the presence of rapakivi textures in the map area (Figure 3b), which are thought to require H_2O-undersatured conditions to form (Nekvasil, 1991). However, the diagram also reveals that for all moderately anhydrous bulk compositions (<0.2 mol% H_2O), over which silicate melt would not be stabilized at <800°C, both orthopyroxene and magnetite (blue line) stability are sensitive to MH_2O. Therefore, in addition to the effects of regional P-T variations discussed above, subtle changes in the water content of a typical granitoid composition at the same P-T condition could also have contributed to the noted discontinuous stability of both phases.

In order to determine the effects of XFe^{3+} on the assemblage, a T-XFe^{3+} diagram was constructed at the same midrange pressure (7 kbar), with XFe^{3+} varying from 0.0 to 0.5 (Figure 6c). This diagram reveals that both magnetite (blue line) and orthopyroxene (green line) stabilities are a strong function of XFe^{3+}, such that variation in XFe^{3+} could also have added to the irregular distribution of both phases. The widespread occurrence of magnetite- and orthopyroxene-bearing metagranitoid rocks suggests that moderate values of $XFe^{3+} = 0.05–0.25$ are the most plausible (a range that includes the assumed value of 0.1; white dashed line in Figure 6c), as both phases are then stabilized within the suggested temperature range.

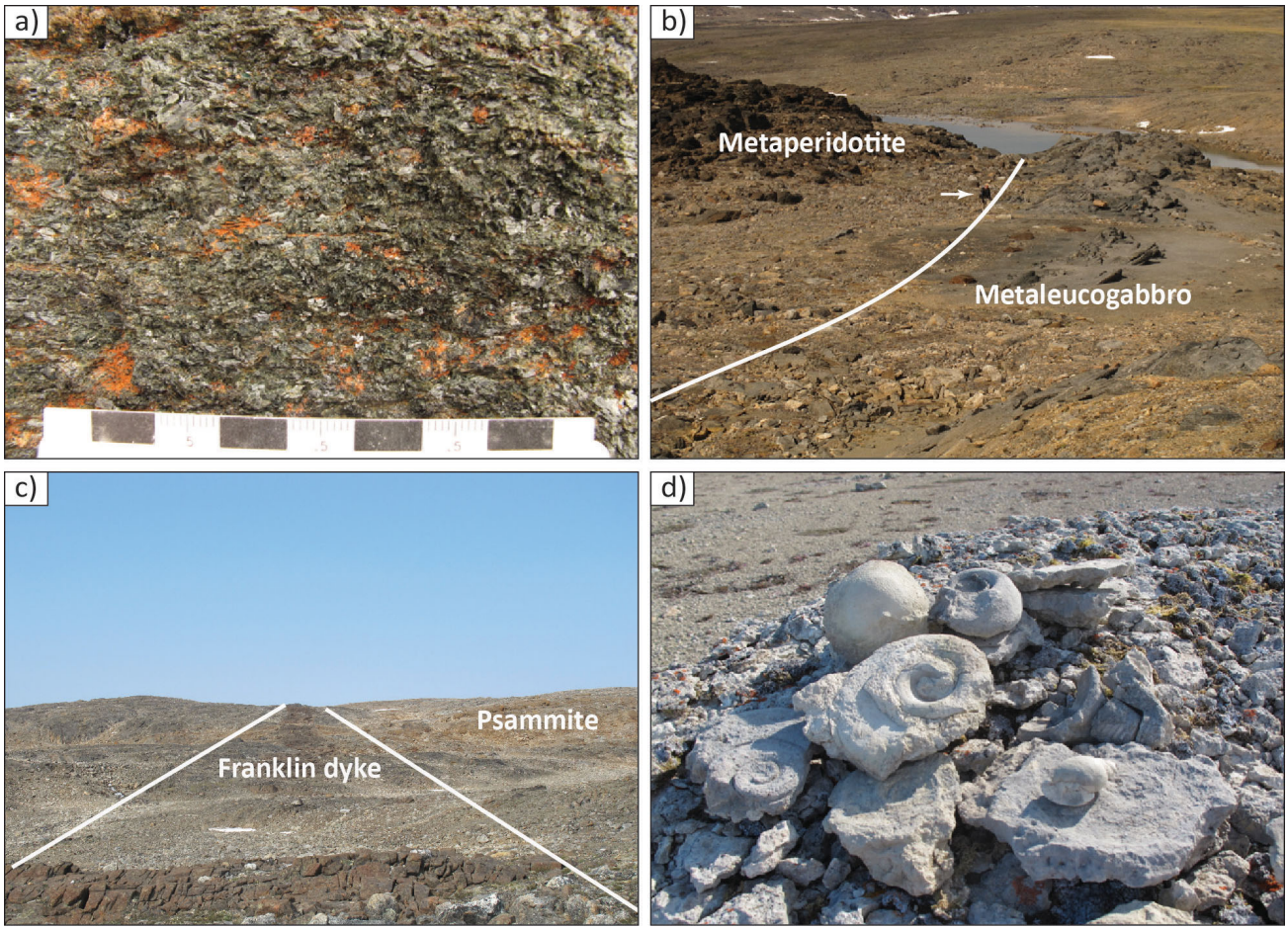

Figure 5: Representative photos of other units on southern Baffin Island: **a)** close-up of metaclinopyroxenite at the base of a layered mafic sill; darker regions correspond to minor retrogression of clinopyroxene to hornblende; **b)** central-upper portion of a layered mafic sill, showing brown-weathering metaperidotite capped by grey-weathering metaleucogabbro (geologist, beside arrow, for scale is 1.8 m tall); **c)** Lake Harbour Group psammite cut by a Franklin dyke, which is approximately 10 m wide and displays columnar jointing in the foreground; **d)** typical knobbly weathered surface of Ordovician limestone, showcasing fossils collected from the wider outcrop; field of view in foreground is 50 cm.

Application to aeromagnetic data

Regional aeromagnetic data show complex variation in the magnetic properties of the bedrock in the project area (e.g., Figure 6d; Kiss and Tschirhart, 2015a, b). Field investigations of the data suggest that the major driver of this variability is the differential abundance of magnetite, typically within otherwise relatively homogeneous plutons (Tschirhart et al., 2015). The phase-equilibria modelling results are consistent with this inference, as they show that subtle changes in P, T and X for a reference granitoid would manifest themselves in complex magnetite (and orthopyroxene) distributions, with all other phases remaining relatively constant.

Regional considerations

The Baffin suture

St-Onge et al. (2007) proposed that a north-dipping, middle Paleoproterozoic suture zone (the Baffin suture of Figure 2) runs through central Baffin Island, approximately along Cumberland Sound, separating the Meta Incognita microcontinent from the Rae craton to the north. Although extensive plutonic activity associated with emplacement of the middle Paleoproterozoic Cumberland Batholith has largely obliterated the older geological record in this locale, two lines of evidence are consistent with the location and vergence of the proposed structure. First, the 'ghost' stratigraphy preserved within the project area changes from dominantly Lake Harbour Group to Piling Group affinity from south to north. On a regional scale, this change in tectonostratigraphic parentage has been previously cited as evidence for an intervening suture zone (St-Onge et al., 2006, 2007). The 2015 field observations thus serve to refine this suggestion, as the most northerly Lake Harbour Group quartzite and southerly Piling Group greywacke constrain a narrow corridor of possible suture-zone loci. Second, a shear zone occurs in the plutonic suite within this corridor, with a top-to-the-south thrust sense of shear. As the emplacement

Table 1: Bulk compositions used to construct all phase-equilibria diagrams in Figure 6 using THERMOCALC (mol %). Two values are provided for Figures 5b and 5c, which represent the end-member compositions of the considered range.

Figure	H_2O	SiO_2	Al_2O_3	CaO	MgO	FeO	K_2O	Na_2O	TiO_2	MnO	O	XFe^{3+}
6a	0.10	79.82	8.79	2.86	0.32	2.14	1.69	3.98	0.16	0.04	0.11	0.1
6b	0.00	79.90	8.79	2.87	0.32	2.14	1.69	3.98	0.16	0.04	0.11	0.1
6b	1.00	79.10	8.71	2.84	0.32	2.12	1.67	3.94	0.16	0.04	0.11	0.1
6c	0.10	79.90	8.80	2.87	0.32	2.14	1.69	3.98	0.16	0.04	0.00	0.0
6c	0.10	79.48	8.75	2.85	0.32	2.13	1.68	3.96	0.16	0.04	0.53	0.5

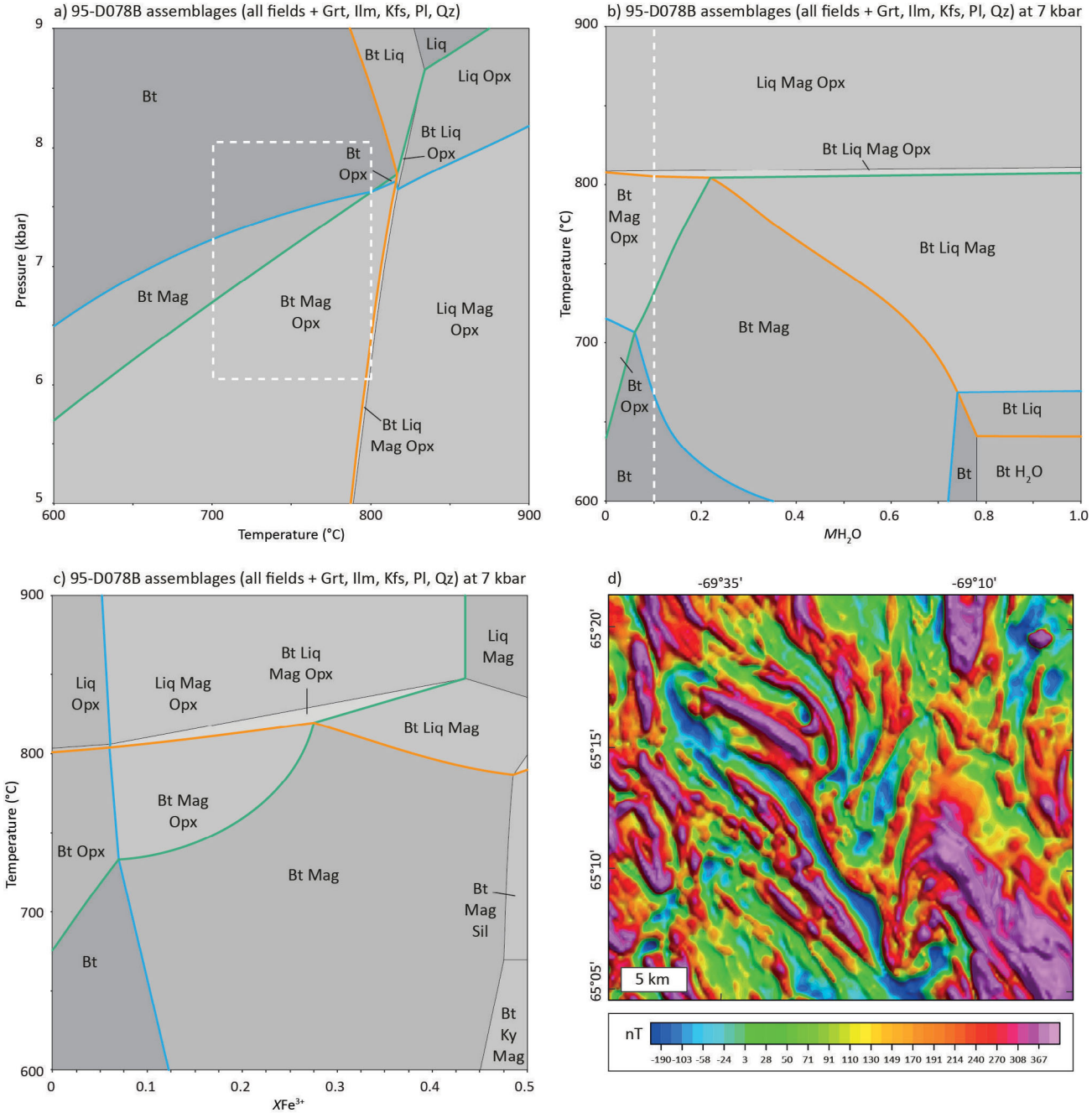

Figure 6: Phase-equilibria modelling of a representative sample of the Cumberland Batholith, southern Baffin Island, exploring metagranitoid amphibolite-granulite facies phase relationships. Phase boundaries (mode = 0 lines) are highlighted for orthopyroxene (green line), magnetite (blue line) and silicate melt (orange line): **a)** P-T diagram; **b)** T-MH_2O diagram; **c)** T-XFe^{3+} diagram; **d)** residual total field over biotite±magnetite±orthopyroxene monzogranite in the western part of the map area. See text for discussion and Table 1 for input bulk compositions. Abbreviations: Bt, biotite; Ky, kyanite; Liq, liquid; Mag, magnetite; Opx, orthopyroxene; Sil, sillimanite.

of the plutonic suite (ca. 1865–1845 Ma; Whalen et al., 2010) postdates the Baffin suture (ca. 1880–1865 Ma; St-Onge et al., 2006), this shear zone could represent reactivation of the suture during prolonged THO deformation.

Future work

Ten new GSC 1:100 000 scale bedrock Canadian Geoscience Map sheets stemming from the 2015 work are currently being prepared for public dissemination in the spring of 2016. The maps, which will feature integrated descriptive notes and a common legend, will complete the modern bedrock-map coverage for Baffin Island south of latitude 70°N.

Planned laboratory work in autumn and winter 2015 includes U-Pb zircon geochronology of the metaplutonic suite from south-central Baffin Island to test correlations with the middle Paleoproterozoic Cumberland batholith and to further constrain the tectonostratigraphic parentage of the host metasedimentary rocks. In particular, detrital zircon will be analyzed from a variety of quartzite samples to establish provenance. All analyses will assist in calibrating the legend of the ten new bedrock maps.

Mineral electron-microprobe analyses and phase-equilibria modelling will document the metamorphic pressure and temperature conditions for samples collected from the map area. The results will be integrated with detailed petrographic studies and in situ monazite geochronology to constrain the tectonometamorphic history of south-central Baffin Island, which will assist in further understanding the evolution of the eastern THO.

Economic considerations

A number of lithological associations and occurrences with potential economic implications were identified during the 2015 field season. This includes several instances of sulphide-bearing gossanous metasedimentary rocks; magnetite and semi-precious minerals in marble, for example gem-quality diopside and apatite; layered mafic-ultramafic sills that may host sulphide mineralization; and several serpentinized ultramafic rocks, which may be suitable as carving stone.

Acknowledgments

Energetic and affable field assistance was provided by T. Chadwick, D. Liikane, T. Milton, S. Noble-Nowdluk, and T. Rowe. C. Gilbert and A. Ford are thanked for their careful management of the project data, with the latter also providing valuable support in the field. The authors are extremely grateful to the camp chef D. Guilfoyle for her many wonderful meals. Universal Helicopters, in particular pilots G. Nuttall and G. Hartery, and Kenn Borek Air are thanked for safe and professional air support. N. Shea, S. Dehler, M. Francis and R. Khoun are acknowledged for their management and administrative support. The Polar Continental Shelf Program (PCSP) provided logistical support (PCSP Project 056-15). Additional financial support of this study was provided by the Strategic Investments in Northern Economic Development (SINED) program delivered by the Canadian Northern Economic Development Agency (CanNor). G. Buller and R. Buenviaje are thanked for processing the archival and new data for south-central Baffin Island. The authors are also are grateful to H. Steenkamp and L. Ham for careful and insightful reviews of this paper.

Natural Resources Canada, Earth Science Sector contribution 20150290

References

Blackadar, R.G. 1967: Geological Reconnaissance, southern Baffin Island, District of Franklin; Geological Survey of Canada, Paper 66-47, 32 p. doi:10.4095/100926

Bucher, K. and Frey, M. 2002: Metamorphism of Granitoid Rocks; *in* Petrogenesis of Metamorphic Rocks, p. 329–334.

Clarke, D.B., Cameron, B.I., Muecke, G.K. and Bates, J.L. 1989: Early Tertiary basalts from the Labrador Sea and Davis Strait region; Canadian Journal of Earth Sciences, v. 26, p. 956–968.

Corrigan, D., Pehrsson, S., Wodicka, N. and de Kemp, E. 2009: the Palaeoproterozoic Trans-Hudson Orogen: a prototype of modern accretionary processes; *in* Ancient Orogens and Modern Analogues, J.B. Murphy, J.D. Keppie and A.J. Hynes (ed.), The Geological Society, London, Special Publications, v. 327, p. 457–479. doi:10.1144/SP327.19

Diener, J.F.A and Powell, R. 2010: Influence of ferric iron on the stability of mineral assemblages; Journal of Metamorphic Geology, v. 28, p. 599–613.

Dunphy, J.M. and Ludden, J.N. 1998: Petrological and geochemical characteristics of a Paleoproterozoic magmatic arc (Narsajuaq Terrane, Ungava Orogen, Canada) and comparisons to Superior Province granitoids; Precambrian Research, v. 91, p. 109–142.

Dyck, B.J. and St-Onge, M.R. 2014: Dehydration-melting reactions, leucogranite emplacement and the Paleoproterozoic structural evolution of Hall Peninsula, Baffin Island, Nunavut; *in* Summary of Activities 2013, Canada-Nunavut Geoscience Office, p. 73–84.

Heaman, L.M., LeCheminant, A.N. and Rainbird, R.H. 1992: Nature and timing of Franklin igneous events, Canada: implications for a Late Proterozoic mantle plume and the break-up of Laurentia; Earth and Planetary Science Letters, v. 109, p. 117–131.

Henderson, J.R. 1985: Geology, McBeth Fiord–Cape Henry Kater, District of Franklin, Northwest Territories; Geological Survey of Canada, Map 1605A, scale 1:250 000.

Hoffman, P.F. 1988: United Plates of America, the birth of a craton: Early Proterozoic assembly and growth of Laurentia; Annual Reviews of Earth and Planetary Sciences, v. 16, p. 543–603.

Holland, T.J.B. and Powell, R. 1998: An internally consistent thermodynamic dataset for phases of petrological interest; Journal of Metamorphic Geology, v. 16, p. 309–343.

Kiss, F. and Tschirhart, V. 2015a: Aeromagnetic survey Amittok Lake area, Baffin Island, Nunavut; Geological Survey of Canada, Open Files 7888–7891, scale 1:100 000.

Kiss, F. and Tschirhart, V. 2015b: Aeromagnetic survey McKeand River area, Baffin Island, Nunavut; Geological Survey of Canada, Open Files 7819–7832, scale 1:100 000.

Liikane, D.A., St-Onge, M.R., Kjarsgaard, B.A., Rayner, N.M., Ernst, R.E and Kastek, N. 2015: Frobisher suite mafic, ultramafic and layered mafic-ultramafic sills, southern Baffin Island, Nunavut; *in* Summary of Activities 2015, Canada-Nunavut Geoscience Office, p. 21–32.

Nekvasil, H. 1991: Ascent of felsic magmas and formation of rapakivi; American Mineralogist, v. 76, p. 1279–1290.

Palin, RM., Weller, O.M., Waters, D.J. and Dyck, B. in press: Quantifying geological uncertainty in metamorphic phase equilibria modelling; a Monte Carlo assessment and implications for tectonic interpretations; Geoscience Frontiers, online version of paper, 17 p. doi:10.1016/j.gsf.2015.08.005

Powell, R. and Holland, T.J.B. 2008: On thermobarometry; Journal of Metamorphic Geology, v. 26, p. 155–179.

Rayner, N.M., Sanborn-Barrie, M., Young, M.D. and Whalen, J.B. 2012: U-Pb ages of Archean basement and Paleoproterozoic plutonic rocks, southern Cumberland Peninsula, eastern Baffin Island, Nunavut; Geological Survey of Canada, Current Research 2012-8, 24 p.

Sanford, B.V. and Grant, A.C.A. 2000: Geological framework of the Ordovician system in the southeast Arctic platform, Nunavut; *in* Geology and Paleontology of the southeast Arctic Platform and southern Baffin Island, Nunavut; Geological Survey of Canada Bulletin 557, p. 13–38.

Scott, D.J. 1997: Geology, U-Pb, and Pb-Pb geochronology of the Lake Harbour area, southern Baffin Island: implications for the Paleoproterozoic tectonic evolution of north-eastern Laurentia; Canadian Journal of Earth Sciences, v. 34, p. 140–155.

Scott, D.J. and Wodicka, N. 1998: A second report on the U-Pb geochronology of southern Baffin Island; *in* Geological Survey of Canada, Current Research 1998-F, p. 47–57.

Scott, D.J., St-Onge, M.R., Wodicka, N. and Hanmer, S. 1997: Geology of the Markham Bay–Crooks Inlet area, southern Baffin Island, Northwest Territories; *in* Geological Survey of Canada, Current Research 1997-C, p. 157–166.

St-Onge, M.R., Hanmer, S. and Scott, D.J. 1996: Geology of the Meta Incognita Peninsula, south Baffin Island: tectonostratigraphic units and regional correlations; *in* Geological Survey of Canada, Current Research 1996-C, p. 63–72.

St-Onge, M.R., Scott, D.J., Wodicka, N. and Lucas, S.B. 1998: Geology of the McKellar Bay–Wight Inlet–Frobisher Bay area, southern Baffin Island, Northwest Territories; *in* Geological Survey of Canada, Current Research 1998-C, p. 43–53.

St-Onge, M.R., Scott, D.J. and Lucas, S.B. 2000a: Early partitioning of Quebec: Microcontinent formation in the Paleoproterozoic; Geology, v. 28, p. 323–326.

St-Onge, M.R. Wodicka, N. and Lucas, S.N. 2000b: Granulite- and amphibolite-facies metamorphism in a convergent plate-margin setting: Synthesis of the Quebec-Baffin segment of Trans-Hudson Orogen; Canadian Mineralogist, v. 38, p. 379–398.

St-Onge, M.R., Searle, M.P. and Wodicka, N. 2006: Trans-Hudson Orogen of North America and Himalaya-Karakoram-Tibetan Orogen of Asia: Structural and thermal characteristics of the lower and upper plates; Tectonics, v. 25, TC4006, 22 p. doi:10.1029/2005TC001907

St-Onge, M.R., Wodicka, N. and Ijewliw, O. 2007: Polymetamorphic evolution of the Trans-Hudson Orogen, Baffin Island, Canada: Integration of petrological, structural and geochronological data; Journal of Petrology, v. 48, p. 271–302. doi:10.1093/petrology/eg1060

St-Onge, M.R., Van Gool, J.A.M., Garde, A.A. and Scott, D.J. 2009: Correlation of Archaean and Palaeoproterozoic units between northeastern Canada and western Greenland: constraining the pre-collisional upper plate accretionary history of the Trans-Hudson orogen; *in* Earth Accretionary Systems in Space and Time, P.A. Cawood and A. Kroner, The Geological Society, London, Special Publications, v. 318, p. 193–235. doi:10.1144/SP318.7

Tschirhart, V., St-Onge, M.R. and Weller, O.M. 2015: Preliminary geophysical interpretation of the McKeand River area, southern Baffin Island, Nunavut: insights from gravity, magnetic and geological data; *in* Summary of Activities 2015, Canada-Nunavut Geoscience Office, p. 49–60.

Thériault, R.J., St-Onge, M.R. and Scott, D.J. 2001: Nd isotopic and geochemical signature of the Paleoproterozoic Trans-Hudson Orogen, southern Baffin Island, Canada: implications for the evolution of eastern Laurentia; Precambrian Research, v. 108, p. 113–138.

Weller, O.M., St-Onge, M.R., Searle, M.P., Rayner, N., Waters, D.J., Chung, S.L., Palin, R.M., Lee, Y.H. and Xu, X.W. 2013: Quantifying Barrovian metamorphism in the Danba Structural Culmination of eastern Tibet; Journal of Metamorphic Geology, v. 31, p. 909–935. doi:10.1111/jmg.12050

Weller, O.M., St-Onge, M.R., Rayner, N., Searle, M.P. and Waters, D.J. in press: Miocene magmatism in the Western Nyainqentanglha mountains of southern Tibet: an exhumed bright spot?; Lithos, online version of paper, 14 p. doi:10.1016/j.lithos.2015.06.024

Whalen, J.B., Wodicka, N., Taylor, B.E. and Jackson, G.D. 2010: Cumberland batholith, Trans-Hudson Orogen, Canada: Petrogenesis and implications for Paleoproterozoic crustal and orogenic processes; Lithos, v. 117, p. 99–118. doi:10.1016/j.lithos.2010.02.008

Wodicka, N. and Scott, D.J. 1997: A preliminary report on the U-Pb geochronology of the Meta Incognita Peninsula, southern Baffin Island, Northwest Territories; *in* Geological Survey of Canada, Current Research 1997-C, p. 167–178.

Wodicka, N., St-Onge, M.R., Corrigan, D., Scott, D.J. and Whalen, J.B. 2014: Did a proto-ocean basin form along the southeastern Rae cratonic margin? Evidence from U-Pb geochronology, geochemistry (Sm-Nd and whole-rock), and stratigraphy of the Paleoproterozoic Piling Group, northern Canada; GSA Bulletin, v. 126, p. 1625–1653. doi:10.1130/B31028.1

Appendix 1 – References cited in Figure 1

1. Blackadar, R.G. 1967: Geology, Cumberland Sound, District of Franklin, Northwest Territories; Geological Survey of Canada, Preliminary Map 17-1966, scale 1:506 880.
2. Blackadar, R.G. 1970: Nottingham, Salisbury, and Mill Islands, District of Franklin, Northwest Territories; Geological Survey of Canada, Preliminary Map 1205A, scale 1:250 000.
3. Jackson, G.D. 1971: Operation Penny Highlands, south-central Baffin Island; Geological Survey of Canada Paper 71-1, Part A, p. 138–140.
4. Trettin, H.P. 1975: Lower Paleozoic geology, central and eastern parts of Foxe Basin and Baird Peninsula, Baffin Island, District of Franklin, Northwest Territories; Geological Survey of Canada, Map 1406A, scale 1:500 000.
5. Morgan, W.C. 1982: Geology, Koch Island, District of Franklin, Northwest Territories; Geological Survey of Canada, Map 1535A, scale 1:250 000.
6. Henderson, J.R. 1985a: Geology, McBeth Fiord-Cape Henry Kater, District of Franklin, Northwest Territories; Geological Survey of Canada, Map 1605A, scale 1:250 000.
7. Henderson, J.R. 1985b: Geology, Ekalugad Fiord-Home Bay, District of Franklin, Northwest Territories; Geological Survey of Canada, Map 1606A, scale 1:250 000.
8. Jackson, G.D. 1998: Geology, Okoa Bay-Padloping Island area, District of Franklin, Northwest Territories; Geological Survey of Canada, Open File 3532, scale 1:250 000.
9. St-Onge, M.R., Scott, D.J. and Wodicka, N. 1999a: Geology, Frobisher Bay, Nunavut; Geological Survey of Canada, "A" Series Map 1979A, 1:100 000 scale. doi:10.4095/210833
10. St-Onge, M.R., Scott, D.J. and Wodicka, N. 1999b: Geology, Hidden Bay, Nunavut; Geological Survey of Canada, "A" Series Map 1980A, 1:100 000 scale. doi:10.4095/210835
11. St-Onge, M.R., Scott, D.J. and Wodicka, N. 1999c: Geology, McKellar Bay, Nunavut; Geological Survey of Canada, "A" Series Map 1981A, 1:100 000 scale. doi:10.4095/210836
12. St-Onge, M.R., Scott, D.J. and Wodicka, N. 1999d: Geology, Wright Inlet, Nunavut; Geological Survey of Canada, "A" Series Map 1982A, 1:100 000 scale. doi:10.4095/210840
13. St-Onge, M.R., Scott, D.J. and Wodicka, N. 1999e: Geology, Blandford Bay, Nunavut; Geological Survey of Canada, "A" Series Map 1983A, 1:100 000 scale. doi:10.4095/210837
14. St-Onge, M.R., Scott, D.J. and Wodicka, N. 1999f: Geology, Crooks Inlet, Nunavut; Geological Survey of Canada, "A" Series Map 1984A, 1:100 000 scale. doi:10.4095/210838
15. St-Onge, M.R., Scott, D.J. and Wodicka, N. 1999g: Geology, White Strait, Nunavut; Geological Survey of Canada, "A" Series Map 1985A, 1:100 000 scale. doi:10.4095/210839
16. Sanford, B.V. and Grant, A.C. 2000: Geological framework of the Ordovician system in the southeast Arctic platform, Nunavut; in Geology and Paleontology of the southeast Arctic Platform and southern Baffin Island, Nunavut; Geological Survey of Canada Bulletin 557, p. 13–38.
17. Jackson, G.D. 2002: Geology, Isurtuq River-Nedlukseak Fiord, Nunavut; Geological Survey of Canada, Open File 4259, scale 1:250 000.
18. St-Onge, M.R., Scott, D.J., Corrigan, D., and Wodicka, N. 2005a: Geology, Ikpik Bay, Baffin Island, Nunavut; Geological Survey of Canada Map 2077A, 1:100 000 scale.
19. St-Onge, M.R., Scott, D.J., Corrigan, D., and Wodicka, N. 2005b: Geology, Flyway Lake, Baffin Island, Nunavut; Geological Survey of Canada Map 2078A, 1:100 000 scale.
20. St-Onge, M.R., Scott, D.J., Corrigan, D., and Wodicka, N. 2005c: Geology, Clyde River, Baffin Island, Nunavut; Geological Survey of Canada Map 2079A, 1:100 000 scale.
21. St-Onge, M.R., Scott, D.J., Corrigan, D., and Wodicka, N. 2005d: Geology, Piling Bay, Baffin Island, Nunavut; Geological Survey of Canada Map 2080A, 1:100 000 scale.
22. St-Onge, M.R., Scott, D.J., Corrigan, D., and Wodicka, N. 2005e: Geology, Straits Bay, Baffin Island, Nunavut; Geological Survey of Canada Map 2081A, 1:100 000 scale.
23. St-Onge, M.R., Scott, D.J., Corrigan, D., and Wodicka, N. 2005f: Geology, Dewar Lakes, Baffin Island, Nunavut; Geological Survey of Canada Map 2082A, 1:100 000 scale.
24. Jackson, G.D. 2006: Geology, Hantzsch River area, Baffin Island, Nunavut; Geological Survey of Canada, Open File 4202, scale 1:250 000.
25. St-Onge, M.R., Sanborn-Barrie, M., and Young, M. 2007a: Geology, Mingo Lake, Baffin Island, Nunavut; Geological Survey of Canada Open File Map 5433, 1:250 000 scale.
26. St-Onge, M.R., Sanborn-Barrie, M., and Young, M. 2007b: Geology, Foxe Peninsula, Baffin Island, Nunavut; Geological Survey of Canada Open File Map 5434, 1:250 000 scale.
27. Sanborn-Barrie, M., Young, M., Whalen, J. and James, D. 2011a: Geology, Ujuktuk Fiord, Nunavut; Geological Survey of Canada, Canadian Geoscience Map 1, (ed. 2, prelim.) 2011; 1 sheet, 1 CD-ROM. doi:10.4095/289237
28. Sanborn-Barrie, M., Young, M. and Whalen, J. 2011b: Geology, Kingnait Fiord, Nunavut; Geological Survey of Canada, Canadian Geoscience Map 2, (ed. 2, prelim.) 2011; 1 , 1 CD-ROM. doi:10.4095/289238
29. Sanborn-Barrie, M., Young, M., Whalen, J., James, D. and St-Onge, M.R. 2011c: Geology, Touak Fiord, Nunavut; Geological Survey of Canada, Canadian Geoscience Map 3 (ed. 2, prelim.), 1 sheet, 1 CD-ROM. doi:10.4095/289239
30. Sanborn-Barrie, M., and Young, M. 2013a: Geology, Circle Lake, Nunavut; Geological Survey of Canada, Canadian Geoscience Map 5 (ed. prelim.), scale 1:100 000; 1 sheet, 1 CD-ROM. doi:10.4095/288929
31. Sanborn-Barrie, M., Young, M., Keim, R., and Hamilton, B.M. 2013b: Geology, Sunneshine Fiord, Nunavut; Geological Survey of Canada, Canadian Geoscience Map 6 (ed. prelim.), scale 1:100 000; 1 sheet, 1 CD-ROM. doi:10.4095/288931
32. Sanborn-Barrie, M. and Young, M. 2013c: Geology, Padle Fiord, Nunavut; Geological Survey of Canada, Canadian Geoscience Map 37 (ed. prelim.), scale 1:100 000, 1 sheet, 1 CD-ROM. doi:10.4095/292014
33. Sanborn-Barrie, M. and Young, M. 2013d: Geology, Durban Harbour, Nunavut; Geological Survey of Canada, Canadian Geoscience Map 38 (ed. prelim.), scale 1:100 000, 1 sheet, 1 CD-ROM. doi:10.4095/292015
34. Sanborn-Barrie, M., and Young, M. 2013e: Geology, Qikiqtarjuaq, Nunavut; Geological Survey of Canada, Canadian Geoscience Map 39 (ed. prelim.), scale 1:100 000, 1 sheet, 1 CD-ROM. doi:10.4095/292016
35. Jackson, G.D. and Sanborn-Barrie, M. 2014: Geology, Pangnirtung Fiord, Nunavut; Geological Survey of Canada,

Canadian Geoscience Map 4 (ed. prelim.), 1:100 000 scale, 1 sheet. doi:10.4095/288928

36. St-Onge, M.R ., Rayner, N.M., Steenkamp, H.M., and Gilbert, C. 2015a: Geology, Terra Nivea, Baffin Island, Nunavut; Geological Survey of Canada , Canadian Geoscience Map 215E (preliminary); Canada-Nunavut Geoscience Office, Open File Map 2015-02E, scale 1:100 000. doi:10.4095/296104
37. St-Onge, M.R., Rayner, N.M., Steenkamp, H.M., and Gilbert, C. 2015b: Geology, Pritzler Harbour, Baffin Island, Nunavut; Geological Survey of Canada, Canadian Geoscience Map 216E (preliminary); Canada-Nunavut Geoscience Office, Open File Map 2015-03E, scale 1:100 000. doi:10.4095/296109
38. St-Onge, M.R., Rayner, N.M., Steenkamp, H.M., and Gilbert, C. 2015c: Geology, Grinnell Glacier, Baffin Island, Nunavut; Geological Survey of Canada, Canadian Geoscience Map 217E (preliminary); Canada-Nunavut Geoscience Office, Open File Map 2015-04E, scale 1:100 000. doi:10.4095/296111
39. Steenkamp, H.M., Gilbert, C., and St-Onge, M.R. 2016a: Geology, Loks Land, Baffin Island, Nunavut, NTS 25-I (part); Geological Survey of Canada, Canadian Geoscience Map 264 (preliminary); Canada-Nunavut Geoscience Office, Open File Map 2016-01, scale 1:100 000. doi:10.4095/297344
40. Steenkamp, H.M., Gilbert, C. and St-Onge, M.R. 2016b: Geology, Ward Inlet (south), Baffin Island, Nunavut,NTS 25-O (south) and 25-J (part); Geological Survey of Canada, Canadian Geoscience Map 266 (preliminary); Canada-Nunavut Geoscience Office, Open File Map 2016-02, scale 1:100 000. doi:10.4095/297349
41. Steenkamp, H.M., Gilbert, C., and St-Onge, M.R. 2016c: Geology, Ward Inlet (north), Baffin Island, Nunavut, NTS 25-O (north); Geological Survey of Canada, Canadian Geoscience Map 265 (preliminary); Canada-Nunavut Geoscience Office, Open File Map 2016-03, scale 1:100 000. doi:10.4095/297348
42. Steenkamp, H.M., Gilbert, C., St-Onge, M.R. 2016d: Geology, Beekman Peninsula (south), Baffin Island, Nunavut, NTS 25-P (south) and 15-M (part); Geological Survey of Canada, Canadian Geoscience Map 267 (preliminary); Canada-Nunavut Geoscience Office, Open File Map 2016-04, scale 1:100 000. doi:10.4095/297351
43. Steenkamp, H.M., Gilbert, C., and St-Onge, M.R. 2016e: Geology, Beekman Peninsula (north), Baffin Island, Nunavut, NTS 25-P (north) and 15-M (part); Geological Survey of Canada, Canadian Geoscience Map 268 (preliminary); Canada-Nunavut Geoscience Office, Open File Map 2016-05, scale 1:100 000. doi:10.4095/297352
44. Steenkamp, H.M., Gilbert, C., and St-Onge, M.R. 2016f: Geology, Leybourne Islands (south), Baffin Island, Nunavut, NTS 26-A (south); Geological Survey of Canada, Canadian Geoscience Map 269 (preliminary); Canada-Nunavut Geoscience Office, Open File Map 2016-06, scale 1:100 000. doi:10.4095/297353
45. Steenkamp, H.M., Gilbert, C., and St-Onge, M.R. 2016g: Geology, Leybourne Islands (north), Baffin Island, Nunavut, NTS 26-A (north); Geological Survey of Canada, Canadian Geoscience Map 271 (preliminary); Canada-Nunavut Geoscience Office, Open File Map 2016-07, scale 1:100 000. doi:10.4095/297355
46. Steenkamp, H.M., Gilbert, C., and St-Onge, M.R. 2016h: Geology, Chidliak Bay (south), Baffin Island, Nunavut, NTS 26-B (south); Geological Survey of Canada, Canadian Geoscience Map 272 (preliminary); Canada-Nunavut Geoscience Office, Open File Map 2016-08, scale 1:100 000. doi:10.4095/297357
47. Steenkamp, H.M., Gilbert, C., and St-Onge, M.R. 2016i: Geology, Chidliak Bay (north), Baffin Island, NTS 26-B (north); Geological Survey of Canada, Canadian Geoscience Map 270 (preliminary); Canada-Nunavut Geoscience Office, Open File Map OFM2016-09, scale 1:100 000. doi:10.4095/297354